LASER INTERFEROMETER GRAVITATIONAL WAVE OBSERVATORY
- LIGO -
CALIFORNIA INSTITUTE OF TECHNOLOGY
MASSACHUSETTS INSTITUTE OF TECHNOLOGY

Document Type	**LIGO-T960139-00 -**	**D**	13Mar96

Shot noise sensitivity of the length control error signals

P Fritschel

Distribution of this draft:

Detector ISC group

This is an internal working note
of the LIGO Project..

California Institute of Technology
LIGO Project - MS 51-33
Pasadena CA 91125
Phone (818) 395-2129
Fax (818) 304-9834
E-mail: info@ligo.caltech.edu

Massachusetts Institute of Technology
LIGO Project - MS 20B-145
Cambridge, MA 01239
Phone (617) 253-4824
Fax (617) 253-7014
E-mail: info@ligo.mit.edu

WWW: http://www.ligo.caltech.edu/

LIGO-DRAFT

1 Overview

This document describes the method used for calculating the shot-noise limited sensitivity of the four interferometric lengths in the LIGO interferometer. The approach is to use analytical expressions for the signals generated by a length (or phase) change; the effect of mirror distortions is included by incorporating the results of FFT analysis in a way described below.

Results are given for the current set of optical parameters and required level of optical distortion. The treatment is made for the single frequency scheme of modulation.

Figure 1 defines the lengths and signals in the interferometer.

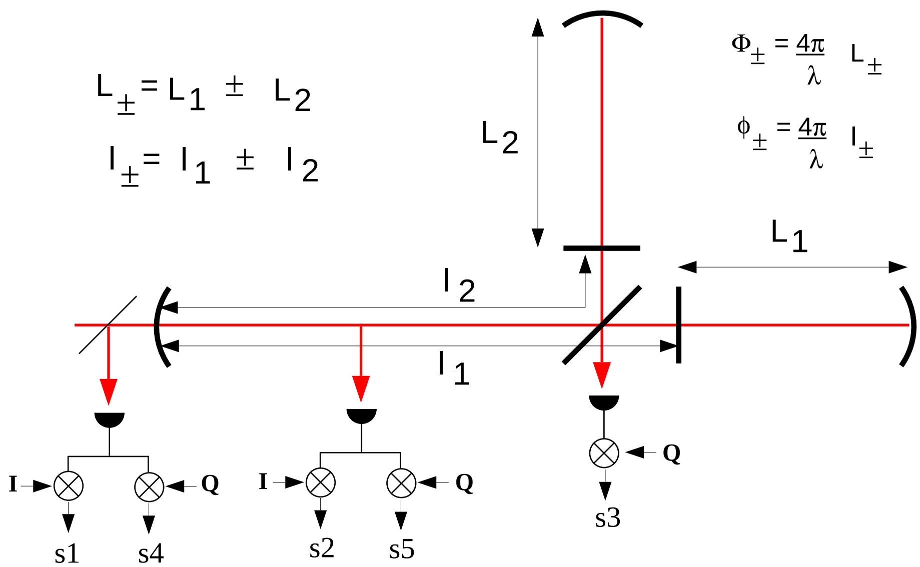

Figure 1. Interferometer configuration

2 Demodulator signals

The following assumptions/approximations are taken for the calculation of the demodulator signals (the derivatives of the demodulators with respect to the various lengths):

- the rf sidebands are resonant in the recycling cavity, but anti-resonant in the arm cavities
- only the beating between the carrier and the first order (upper and lower) sidebands is considered
- only the signals at DC are computed
- only the TEM_{00} components of the carrier and sideband fields - as given by the FFT results - contribute to the signal
- the photocurrents are sine/cosine- demodulated
- Units: the power levels (P_0) are to be expressed in units of (# photons/sec); the expressions which follow then give (# photo-electrons/sec/ phase shift), assuming a quantum efficiency (QE) of one. Less-than-unity-QE is included by multiplying the expressions by the

LIGO-DRAFT

QE.

The expressions for the demodulator derivatives are the same as found in M Regehr's thesis, with the stipulation that only the TEM_{00} components are considered. Definitions for the various symbols are found in Appendix 1, Table 3.

2.1. Differential degrees of freedom

Signal at s_3: The signal at s_3 is the gw signal; it is mostly sensitive to $\Phi\_ / L\_$, but is also sensitive to $\phi\_ / l\_$:

$$\frac{ds_3}{d\Phi\_} = P_0 \cdot J_0(m) \cdot J_1(m) \cdot \left(\frac{E^c_{rec}}{E^c_i}\right)\left(\frac{E^{sb}_{anti}}{E^{sb}_i}\right) \cdot \left|r^c_{cav}{}'\right|$$

$$= P_0 \cdot J_0(m) \cdot J_1(m) \cdot \sqrt{G^c_{rec} \cdot T^{sb}_{anti}} \cdot G^c_{cav}$$

$$\frac{ds_3}{d\phi\_} = P_0 \cdot J_0(m) \cdot J_1(m) \cdot \left(\frac{E^c_{rec}}{E^c_i}\right)\left(\frac{E^{sb}_{anti}}{E^{sb}_i}\right) \cdot r^c_{cav}$$

$$= P_0 \cdot J_0(m) \cdot J_1(m) \cdot \sqrt{G^c_{rec} \cdot T^{sb}_{anti}} \cdot r^c_{cav}$$

Signal at s4: The signal at s_4 is mainly sensitive to $\phi\_ / l\_$, but also has some sensitivity to $\Phi\_ / L\_$:

$$\frac{ds_4}{d\phi\_} = P_0 \cdot J_0(m) \cdot J_1(m) \cdot t_p \left(\frac{E^c_{ref}}{E^c_i}\right)\left(\frac{E^{sb}_{anti}}{E^{sb}_i}\right)\left(\frac{E^{sb}_{rec}}{E^{sb}_i}\right)$$

$$= P_0 \cdot J_0(m) \cdot J_1(m) \cdot t_p \sqrt{R^c_{ifo} \cdot T^{sb}_{anti} \cdot G^{sb}_{rec}}$$

LIGO-DRAFT

$$\frac{ds_4}{d\Phi_-} = \frac{ds_4}{d\phi_-} \cdot \left| r_{cav}^{sb}{}' \right|$$

$$= P_0 \cdot J_0(m) \cdot J_1(m) \cdot t_p \sqrt{R_{ifo}^c \cdot T_{anti}^{sb} \cdot G_{rec}^{sb}} \cdot G_{cav}^{sb}$$

Signal at s5: The signal at s_5 (quad phase of the recycling cavity signal) is an alternative to s_4; it is mainly sensitive to ϕ_- / l_- :

$$\frac{ds_5}{d\phi_-} = P_0 \cdot J_0(m) \cdot J_1(m) \cdot R_p \left(\frac{E_r^c}{E_i^c} \right) \left(\frac{E_{anti}^{sb}}{E_i^{sb}} \right) \cdot N_1 r_R$$

$$= P_0 \cdot J_0(m) \cdot J_1(m) \cdot \sqrt{G_{rec}^c \cdot G_{rec}^{sb} \cdot T_{anti}^{sb}} \cdot (r_R / t_R)$$

2.2. Common degrees of freedom

Signal at s_1: Assuming all the light reflected from the interferometer is detected (or if not, the following expressions can be multiplied by the suitable fractional detected power), we have:

$$\frac{ds_1}{d\Phi_+} = P_0 \cdot J_0(m) \cdot J_1(m) \cdot \left(\frac{E_{ref}^c}{E_i^c} \right) \left(\frac{E_{ref}^{sb}}{E_i^{sb}} \right) N_0' \left| \frac{r_{cav}^{sb}{}'}{r_{cav}^c} \right|$$

$$= P_0 \cdot J_0(m) \cdot J_1(m) \cdot T_p \sqrt{R_{ifo}^{sb}} \cdot G_{rec}^c \cdot G_{cav}^c$$

$$\frac{ds_1}{d\phi_+} = P_0 \cdot J_0(m) \cdot J_1(m) \cdot \left(\frac{E_{ref}^c}{E_i^c} \right) \left(\frac{E_{ref}^{sb}}{E_i^{sb}} \right) [N_0' - N_1']$$

$$= P_0 \cdot J_0(m) \cdot J_1(m) \cdot T_p [\sqrt{R_{ifo}^{sb}} \cdot G_{rec}^c \cdot r_{cav}^c - \sqrt{R_{ifo}^c} \cdot G_{rec}^{sb} \cdot \cos\alpha]$$

In the above expression, $\cos\alpha$ and $r^c{}_{cav}$ are determined from the TEM_{00} power levels as follows:

$$\cos\alpha = \sqrt{P_{symm}^{sb} / P_{rec}^{sb}}$$

$$r_{cav}^c = \sqrt{P_{symm}^c / P_{rec}^c}$$

Signal at s_2 : This is the signal from the recycling cavity field. In M Regehr's thesis, this is taken from the symmetric port of the beamsplitter; in LIGO this beam would be taken from one (or both) of the beams reflected from the input test mass AR surfaces, which is a sample of the beam

LIGO-DRAFT

traveling toward the beamsplitter. This field is normally called the recycling cavity field, and is only slightly different than the symmetric port field. The following expression are thus slightly different from those in MR's thesis:

$$\frac{ds_2}{d\Phi}_+ = P_0 \cdot J_0(m) \cdot J_1(m) \cdot R_p \left(\frac{E^c_{rec}}{E^c_i}\right)\left(\frac{E^{sb}_{rec}}{E^{sb}_i}\right) N_0 \cdot r_R T_p \left|r^c_{cav}{}'\right|$$

$$= P_0 \cdot J_0(m) \cdot J_1(m) \cdot R_p \sqrt{G^{sb}_{rec}} \cdot G^c_{rec} \cdot G^c_{cav} \cdot T_p (r_R / t_R)$$

$$\frac{ds_2}{d\phi}_+ = P_0 \cdot J_0(m) \cdot J_1(m) \cdot R_p \left(\frac{E^c_{rec}}{E^c_i}\right)\left(\frac{E^{sb}_{rec}}{E^{sb}_i}\right) r_R T_p [N_0 r^c_{cav} - N_1 \cos\alpha]$$

$$= P_0 \cdot J_0(m) \cdot J_1(m) \cdot R_p \sqrt{G^c_{rec} G^{sb}_{rec}} \cdot T_p (r_R / t_R) [r^c_{cav} \sqrt{G^c_{rec}} - \cos\alpha \sqrt{G^{sb}_{rec}}]$$

In the above, the values of the pick-off and recycling mirror parameters (R_p , T_p , r_R , t_R) are taken to be their nominal ones (assumed to be lossless).

3 Shot noise

The beating of the carrier with the sidebands produces shot noise in the I and Q phases at the modulation frequency on the photodetectors. The shot noise in these photocurrents after demodulation (n_i) will be expressed in terms of a spectral density measured at the demodulator outputs defined above (s_i); the units of n_i are thus (#/sec/√Hz). Taking into account the non-stationarity of the photocurrents being demodulated, the expressions for the shot noise of the five demodulated signals are:

$$n_1, n_2, n_3 = \sqrt{P_c + \frac{3}{2} P_{sb}} \cdot \sqrt{\frac{\eta}{h\nu}}$$

$$n_4, n_5 = \sqrt{P_c + \frac{1}{2} P_{sb}} \cdot \sqrt{\frac{\eta}{h\nu}}$$

where η is the detector's quantum efficiency, P_c is the total carrier power (all modes) and P_{sb} is the total sideband power (all modes, both sidebands). In each case, the power levels at the port in

LIGO-DRAFT

question are to be used in the expressions (e.g., to compute n_3, the power levels at the anti-symmetric port are inserted).

4 Shot noise sensitivities

A Mathematica Notebook has been written to compute the signals, noise, and signal-to-noise ratios using the above expressions. The notebook is found in: *~pf/ifoconfig/shotnoise/shotnoise_v2.ma* .

The error signals have frequency dependencies which have not been included here; this means there is also a frequency dependence to the shot noise sensitivity of each error signal. The approach of this modeling effort has been to get realistic values for the noise and DC signals by combining FFT results with analytical expressions. The frequency dependence can then be incorporated by using the results of a frequency response model such as Twiddle, which is a plane wave model (no mirror distortions). It is not expected that the frequency response (i.e., locations of poles and zeros) is significantly affected by the mirror distortions (this has been verified for the gw signal).

Some of the signals depend critically on the recycling mirror reflectivity, the asymmetry, and the losses in the interferometer. In the near future (~1 month), an exploration of the asymmetry-Trec parameter space will be made using the FFT and a given set of mirror distortions. For the moment, I present the shot noise sensitivities using the results of a single FFT run.

Parameters of the FFT run: The FFT data used was made using: ‘lambda/400’ surfaces; 50 ppm loss per optic; 30 cm aperture optics; 1.064 micron light. The recycling mirror transmission was fixed at 4.0%. This was important to keep the carrier (TEM_{00}) reflected power from the interferometer from being too small (the ‘optimized’ transmission was 3.33%). In fact it was found that the strain sensitivity (sensitivity to L_-) was very slightly better with this choice of recycling mirror transmission than for the previously ‘optimized’ case; this is because the sideband transmission to the dark port becomes more efficient with the lower recycling cavity finesse.

Additional parameters: The following additional parameters were used to obtain the shot noise sensitivities which follow: P_{in} = 5 W; PD quantum efficiency = 0.8; pick-off reflectivity for detection of s2 and s5 signals = 0.001; pick-off reflectivity for detection of s1 and s4 signals = 1.0.

Shot noise sensitivities: The shot noise sensitivities of the five error signals to the degree of freedom they are intended to control (at DC) are shown in Table 1. The sensitivity number represents the motion of the d.o.f. under question (in m/√Hz) required to produce a signal equal to the shot noise on the error signal under question. For s1 and s2, the shot noise sensitivities to the d.o.f. not being controlled are also shown. The sensitivities are shown for two cases: where the modulation

LIGO-DRAFT

index has been optimized for the gw signal (s3); where the modulation index is optimized for that particular d.o.f.

Table 1:

Signal	*Degree-of-freedom*	*Sensitivity when modulation optimized for gw (m=0.47)*	*Sens. (m) when modulation optimized for each case*
s1	$\mathbf{L_+}$	$\mathbf{2.21 \times 10^{-20}}$ **m/√Hz**	2.04×10^{-20} (m=0.74)
	l_+	5.03×10^{-18} m/√Hz	
s2	$\mathbf{l_+}$	$\mathbf{1.10 \times 10^{-16}}$ **m/√Hz**	6.86×10^{-17} (m=1.13)
	L_+	1.79×10^{-19} m/√Hz	
s3	$\mathbf{L_-}$	$\mathbf{5.20 \times 10^{-20}}$ **m/√Hz**	
s4	$\mathbf{l_-}$	$\mathbf{2.48 \times 10^{-17}}$ **m/√Hz**	1.96×10^{-17} (m=0.90)
s5	$\mathbf{l_-}$	$\mathbf{1.31 \times 10^{-16}}$ **m/√Hz**	6.84×10^{-17} (m=1.34)

The strain sensitivity corresponding to the s3 sensitivity is $h(0) = 1.30 \times 10^{-23}$ /√Hz. The sensitivity to frequency noise at s1 implied by the above value is $\delta\nu(0) = 7.78 \times 10^{-10}$ Hz/√Hz.

Table 2 shows the individual signal and noise values for a modulation index of m=0.47. The units for the signal are (effective watts/ lambda), expressed in dB (effective watts = watts × quantum efficiency); the units for noise are (#/sec/√Hz).

Table 2:

Detector #	*Signal*	*Noise*
1	$ds1/dL_+$: 75.2 dB	6.37×10^{8}
	$ds1/dl_+$: 28.0 dB	
2	$ds2/dL_+$: 58.9 dB	7.98×10^{8}
	$ds2/dl_+$: 3.2 dB	
3	$ds3/dL_-$: 77.0 dB	1.86×10^{9}
	$ds3/dl_-$: 34.7 dB	
4	$ds3/dL_-$: -30.2 dB	5.05×10^{8}
	$ds3/dl_-$: 12.2 dB	

LIGO-DRAFT

Table 2:

Detector #	*Signal*	*Noise*
5	$ds3/dL_-$: - 41.0 dB	7.70×10^8
	$ds3/dl_-$: 1.3 dB	

APPENDIX 1 SYMBOLS

Table 3 defines the symbols used in the preceding expressions.

Table 3:

Symbol	*Definition*
E_i^c	carrier field incident on the interferometer
E_i^{sb}	sideband field (upper or lower) incident on the ifo
$E^c{}_{rec}$	carrier field in the recycling cavity (traveling toward beam-splitter; TEM_{00} component)
$E^{sb}{}_{rec}$	sideband field (upper or lower) in the recycling cavity (traveling toward beamsplitter; TEM_{00} component)
$E^{sb}{}_{anti}$	sideband field (upper or lower) at the anti-symmetric port (TEM_{00} component)
$E^c{}_{ref}$	carrier field reflected from the ifo (TEM_{00} component)
$E^{sb}{}_{ref}$	sideband field reflected from the ifo (TEM_{00} component)
$G^c{}_{rec}$	recycling cavity power gain for carrier, TEM_{00} component
$G^{sb}{}_{rec}$	recycling cavity power gain for sideband, TEM_{00} component
$G^c{}_{cav}$	arm cavity power gain for carrier, TEM_{00} component
$G^{sb}{}_{cav}$	arm cavity power gain for sideband, TEM_{00} component
N_0	carrier bounce number in recycling cavity (TEM_{00} comp.)
N_1	sideband bounce number in recycling cavity (TEM_{00} comp.)

LIGO-DRAFT

Table 3:

Symbol	*Definition*
N_0'	augmented carrier bounce number in recycling cavity (TEM_{00} comp.)
N_1'	augmented sideband bounce number in recycling cavity (TEM_{00} comp.)
P_0	total input power to ifo
r^c_{cav}	carrier reflectivity of arm cavity on resonance (magnitude; TEM_{00} comp.)
$\|r^c_{cav}{}'\|$	derivative of arm cavity carrier reflectivity w.r.t. round-trip phase shift (on resonance; magnitude; TEM_{00} comp.)
$\|r^{sb}_{cav}{}'\|$	derivative of arm cavity sideband reflectivity w.r.t. round-trip phase shift (carrier resonant; magnitude; TEM_{00} comp.)
r_R	field reflectivity of recycling mirror
R^c_{ifo}	power reflectivity of the resonant interferometer for the carrier, TEM_{00} component
R^{sb}_{ifo}	power reflectivity of the resonant interferometer for the sideband (upper or lower), TEM_{00} component
R_p	power reflectivity of pick-off for sampling recycling cavity field
t_R	field transmission of recycling mirror
t_p , T_p	field and power transmission of recycling cavity pick-off
T^{sb}_{anti}	power transmission of sideband (upper or lower) from ifo input to anti-symmetric port of BS; TEM_{00} component

LIGO-DRAFT